VIA MEDICA

Nuclear Medicine Review 2013, 16, 1: 9–16
10.5603/NMR.2012.0002

ISSN 1506–9680

Original

Optimization of image reconstruction method for SPECT studies performed using [^{99m}Tc-EDDA/HYNIC] octreotate in patients with neuroendocrine tumors

Anna Sowa-Staszczak, Wioletta Lenda-Tracz,
Monika Tomaszuk, Bogusław Głowa,
Alicja Hubalewska-Dydejczyk
Department of Endocrinology, Jagiellonian University Medical College, Krakow, Poland

[Received 6 IV 2012; Accepted 28 XI 2012]

Abstract

BACKGROUND: Somatostatin receptor scintigraphy (SRS) is a useful tool in the assessment of GEP-NET (gastroenteropancreatic neuroendocrine tumor) patients. The choice of appropriate settings of image reconstruction parameters is crucial in interpretation of these images. The aim of the study was to investigate how the GEP NET lesion signal to noise ratio (TC_S/TC_B) depends on different reconstruction settings for Flash 3D software (Siemens).
METHODS: SRS results of 76 randomly selected patients with confirmed GEP-NET were analyzed. For SPECT studies the data were acquired using standard clinical settings 3–4 h after the injection of 740 MBq ^{99m}Tc-[EDDA/HYNIC] octreotate. To obtain final images the OSEM 3D Flash reconstruction with different settings and FBP reconstruction were used. First, the TC_S/TC_B ratio in voxels was analyzed for different combinations of the number of subsets and the number of iterations of the OSEM 3D Flash reconstruction. Secondly, the same ratio was analyzed for different parameters of the Gaussian filter (with FWHM = 2–4 times greater from the pixel size). Also the influence of scatter correction on the TC_S/TC_B ratio was investigated.
RESULTS: With increasing number of subsets and iterations, the increase of TC_S/TC_B ratio was observed. With increasing settings of Gauss [FWHM coefficient] filter, the decrease of TC_S/TC_B ratio was reported. The use of scatter correction slightly decreases the values of this ratio.
CONCLUSIONS: OSEM algorithm provides a meaningfully better reconstruction of the SRS SPECT study as compared to the FBP technique. A high number of subsets improves image quality (images are smoother). Increasing number of iterations gives a better contrast and the shapes of lesions and organs are sharper. The choice of reconstruction parameters is a compromise between image qualitative appearance and its quantitative accuracy and should not be modified when comparing multiple studies of the same patient.
KEY words: OSEM, SPECT, SRS, GEP-NET

Nuclear Med Rev 2013; 16, 1: 9–16

Correspondence to: Wioletta Lenda Tracz Ph.D
Department of Endocrinology, Jagiellonian University Medical College, Krakow, Poland
ul. Kopernika 17, 31–501 Krakow, Poland
Tel: +48 12 424 75 12
Fax: +48 12 424 73 99
e-mail: wioletta.tracz@gmail.com

Background

Somatostatin receptor scintigraphy (SRS) with the use of labeled somatostatin analogs plays an important role in the diagnosis and therapy of neuroendocrine tumors (NETs) and their metastases. Because of its high sensitivity and specificity, SRS is often the method of choice in diagnosis of these tumors compared to other conventional imaging techniques such as ultrasonography (USG), computed tomography (CT) or magnetic resonance imaging (MRI). Somatostatin receptor scintigraphy is considered to be useful for several clinical indications: the localization of primary tumor, the evaluation of disease extension (staging) and the qualification for peptide receptor radionuclide therapy (PRRT). Because receptor expression on the surface of lesion cellular membranes can be

directly correlated with the intensity of the radiopharmaceutical uptake [1] this uptake in lesions is a significant indicator in therapy stratification with the use of somatostatin analogs labeled with ^{90}Y or/and ^{177}Lu [2–8].

An optimized method of single photon emission computed tomography (SPECT) image reconstruction is crucial to the interpretation of SRS images of NETs. A few years ago iterative methods of SPECT images reconstruction were not as common as today. Because of increased computer power, commercial software with implemented iterative reconstruction methods, such as ordered subsets expectation maximization (OSEM), were introduced into clinical practice. Nowadays OSEM [9] has become the most important iterative reconstruction technique in SPECT studies. But the choice of appropriate sets of parameters for OSEM algorithm (subsets number and iterations number for defined number of subsets) may significantly influence the quality of reconstructed images and clinical assessment of lesion signal to noise ratio (TC_S/TC_B ratio — Total $Counts_{Signal}$/Total $Counts_{Background}$ ratio) [10].

There is still limited number of publications concerning the optimization of iterative algorithms applied to the reconstruction of SPECT images of NETs. Most of them were phantom studies. This subject was also investigated in several experiments and clinical trials referred to other diseases, mainly as a comparison of two techniques of images reconstruction (FBP versus iterative algorithms: maximum likelihood expectation maximization (MLEM) or/and OSEM) [11–16].

The [^{99m}Tc-EDDA/HYNIC]octreotate labeled somatostatin analog improves the diagnostic efficacy of gastroenteropancreatic neuroendocrine tumors (GEP-NET) in localization of primary tumors and their metastases. Currently SRS is the most important study when making a decision about the use of PRRT. Nowadays, this model of therapy is considered to be an effective treatment in inoperable and diffuse NETs. Optimization of the method of reconstruction of SPECT images is necessary to increase the sensitivity and specificity of SRS study.

The aim of the present study was to optimize the OSEM iterative method of reconstruction of SRS SPECT images obtained from the scans performed in patients with neuroendocrine tumors. To this end, an investigation of the Flash 3D™ software available on several models of the Siemens cameras (Siemens Healthcare) was performed. Authors also compared the effectiveness of the two reconstruction techniques: the older, but still commonly used FBP versus the optimized OSEM iterative technique (OSEM Flash 3D™).

Material and methods

The SRS results for a group of 76 randomly selected patients with GEP-NET (42 females and 34 males, age: 60.0 ± 11.6 years) were analyzed. In each case, GEP-NET was confirmed in a histopathological examination and lesions were localized with the use of other conventional diagnostic studies (USG, CT, MRI or endoscopy studies). A total of 197 lesions (108 lesions localized in the liver and 89 lesions with an out-liver localization) were analyzed.

Image acquisition

SPECT studies were performed with the use of a dual head gamma camera (E.CAM 180, Siemens Healthcare) equipped with a low energy high resolution (LEHR) collimators. Each study was performed 3-4 hours after the intravenous injection of 740 MBq of [^{99m}Tc-EDDA/HYNIC]octreotate. Data acquisitions were performed using a 180° noncircular orbit and a total of 128 projections angles (30 seconds per projection), 128 × 128 matrix size, zoom 1.23 and 3.9 mm pixel size. A symmetrical 15% wide energy window for the acquisition was centered at 140 keV. The second window placed below, also 15% wide, was added for scatter correction (SC) using dual energy window method. The standard Chang attenuation correction was applied to reconstructed slices. In this technique, an ellipse is generated based on patient (or phantom) transaxial slice and a constant linear attenuation coefficient of the medium μ is applied to the reconstructed image [17]. The linear attenuation correction was set to $\mu = 0.15$ cm^{-1}.

The software SPECT with CT study fusion (SPECT and CT images performed on different equipment) was performed to verify the localization of each lesion described in SPECT images.

Image processing

Each SPECT image was reconstructed with the use of iterative technique including depth-dependent 3-dimensional resolution recovery (OSEM Flash 3D™). The scheme of the optimization of SPECT images with the use of OSEM technique included 34 different settings of reconstruction parameters. Based on the results obtained at each step of optimization, the next step was always a consequence of the results of the previous one. The analysis was performed in consecutive phases: **phase 1** — the analysis with variable number of subsets (s = 8, 16, 32) and variable number of iterations (i = 2–7), **phase 2** — the analysis with constant number of subsets (s = 8) and variable number of iterations (I = 6–30) with the step equal to 4 iterations, **phase 3** — assessment of the influence of scatter correction for the defined (optimized) number of subsets and iterations (s = 8, I = 10), **phase 4** — evaluation of the Gauss filter utilization (FWHM = n·p [mm]; n = 1, 2, 3, 4; p = 3.9 ≈ 4 [mm]) for optimized reconstruction parameters OSEM (8, 10) with the use of scatter correction, **phase 5** — comparison of two techniques of reconstructions: optimized OSEM versus FBP (with Butterworth, (cutoff frequency $f_c = 0.86$).

Image evaluation

All considered lesions were divided into two groups based on their localization: group I — lesions localized in the liver and group II — lesions with extrahepatic localization (within the abdomen). Additionally, all lesions localized in the liver and outside the liver were divided into two subgroups depending on their volume (VOI, volume of interest). In this case subgroup 1corresponded to small lesions: VOI < 1.6 cm^3, and subgroup 2 to medium size lesions: VOI: 1.6–3.2 cm^3).

Reconstructed images were analyzed in qualitative and quantitative way.

The TC_S/TC_B ratio was used for quantitative assessment of SPECT images. To calculate the TC_S/TC_B ratio for each of the reconstructed images, the lesions were marked as volume of interests (VOIs). VOIs were drawn with the use of multiframe isocontour technique by manually adjusting the threshold of the isocontour in such a way that the VOI boundaries coincided with the very well visible lesion signal for constant color scale intensity for all combinations of parameters setting in every patient study. Values of the thresholds were between 15% and 65% of the maximum voxel

value of the respective VOIs. VOIs volumes varied between 0.59 ml and 3.19 ml. The PET color scale was used. The color intensity varied (15–38%) but was maintained constant for each investigated study and each parameters settings. In each case the background color scale was set at the same level (0%) and the background VOI was drawn similar to the lesion VOI using the same technique as described above. The VOIs of the lesion and of the background localized in this lesion neighborhood had the same volumes and were maintained constant for each investigated combination of the reconstruction parameters.

In parallel, qualitative lesions assessment was performed by determining the intensity (visibility) of tracer uptake for each of the reconstruction settings. The quality of images was estimated by two independent observers according to the two-grade scale: 0 — poorly visible lesion, 1 — very well visible lesion. Moreover, special attention was paid to the lesions location, especially in cases when lesions were situated near large gatherings of activity, such as the spleen and kidneys.

Phantom study

All results of the qualitative analysis were compared with the results of the phantom study. For this purpose a substitute of the Jaszczak phantom with hot spheres was prepared in accordance with data obtained from the clinical part of this study. The cylindrical body of the Jaszczak phantom was used (21 cm diameter, 17 cm high) and five cylindrical containers (syringes with suitable volume) were placed inside the phantom. The volumes activity placed in containers calculated using the method proposed by Brambilla et al. were equal to 0.5; 1.0; 1.5 (2 cm^3 syringes); 2.0 and 3.0 cm^3 (5 cm^3 syringes) [11]. In order to simulate different background activity concentrations the phantom was filled with a uniform ^{99m}Tc solutions of 37 kBq/ml and 4.7 kBq/ml, hereafter referred as high and low background. To introduce different lesions, the five hot volumes were created with lesion-to-background activity ratios of 2:1, 6:1, 10:1, 18:1 and 30:1 for both high and low background activity.

Statistical methods

The logarithmic transformation of TC_S/TC_B ratio results was performed. To determine whether a quantitative data set can be modeled by a normal distribution, the Shapiro-Wilk test was used. If the data were normally distributed, multivariate ANOVA approach for repeated measurements followed by Tuckey test was used. In cases when the data displayed non-Gaussian distribution, the nonparametric ANOVA Friedman test was used. To compare outcomes of the qualitative analyses where variables had only two possible values (coded as 0 — poor visible lesion or 1 — very well visible lesion), non-parametric Cochran's Q test was used.

In all statistical analyses, 95% confidence level was assumed.

Results

The qualitative assessment for different number of subsets and iterations was performed at the first stage of the study (phase 1). For lesions localized in the liver (group I), the highest number of lesions assessed as very well visible (value of 1) was achieved for 8 subsets and different number of iterations (i): OSEM (8, i) (subgroup 1: 54–63%; $p < 0.05$; subgroup 2: 59–86%; $p < 0.05$). Comparable results were obtained for lesions with extrahepatic localization (group II) in subgroup 1 and 2 (6–38% and 54–77%, respectively; $p < 0.05$).

At the next step (phase 2) and based on the outcomes from the phase 1 of this study, the variable number of iterations was investigated for the constant number of subsets [OSEM (8, i)]. In the qualitative assessment, the highest number of lesions localized in the liver (group I) was assessed as very well visible for 10 iterations for both small and medium size lesions (44% and 82%, respectively; $p < 0.05$). Additionally, the same percentage of lesions was assessed as very well visible for 14 and 18 iterations. The similar trend was observed for lesions with extrahepatic localization (group II); $p < 0.05$: small lesions — 35% (OSEM(8,10)) and medium size lesions — 89% [OSEM (8, 10) and OSEM (8, 14)].

When performing quantitative analysis of the data, the mean value of TC_S/TC_B ratio increased with the increasing number of iterations for both localizations: in the liver (Figures 1A and 1B) and outside the liver, within abdomen (Figures 1C and 1D). However for lesions localized in the liver the differences in average values of the TC_S/TC_B ratio were statistically significant for the number of iterations (i) equal to $i = 10$, 14 and 18 for the lesion subgroup 1 ($p < 0.05$); and for the subgroup 2 for $i = 6$, 10 and 14 ($p < 0.05$). For extrahepatic lesions these differences were statistically significant for $i = 6$ and 10 ($p < 0.05$) for both small and medium size lesions.

Scatter correction (SC) applied to the SPECT images reconstruction (phase 3) did not altered qualitative assessment of the lesions localized in the liver. However, for images reconstructed with and without SC small but significant differences in the number of well visible lesions (assessed as 1) were observed for lesions with extrahepatic localization (24% *v.* 15% and 71% *v.* 61% for small and medium size lesions respectively). These differences were not statistically significant for the lesions in the liver (group I). Additionally, it should be highlighted that SC application increased the mean value of TC_S/TC_B ratio in each investigated subgroup.

The Gauss filter application influenced the sharpness of the reconstructed images. The most effective coefficient of Gauss filter was FWHM = 4 mm and 8 mm ($p < 0.05$). These values were approximately equal to the pixel size and the double of the pixel size. For these two values of FWHM parameter the percentage of lesions assessed as very well visible for group I and II was: 22% and 17% (small lesions) and 71% and 79% (medium size lesions), respectively. However, such image smoothing considerably decreased the value of TC_S/TC_B ratio for lesions localized in the liver and outside the liver (within the abdomen). Figure 2 shows the effect of image smoothing with the use of Gauss filter for FWHM = 4 mm and 8 mm.

In the last phase (phase 5) the most effective settings of the OSEM reconstruction were compared to the most common method of reconstruction — FBP. In both investigated groups (I and II), the quality of reconstructed images was significantly superior for the OSEM algorithm versus FBP technique: subgroup 1: 31% *v.* 8% and 15% *v.* 10%, respectively and subgroup 2: 54% *v.* 11% and 82% *v.* 42%, for small and medium size lesions respectively. Differences in a quality assessment of SPECT images were not statistically significant only for small lesions in extrahepatic localization. The mean value of TC_S/TC_B ratio was near 1.5 times higher for optimized setting OSEM (8, 10) with SC *v.* FBP for both size of lesions localized in the liver (Figures 3A and 3B) and outside the liver localization (Figures 3C and 3D). Figure 4 shows differences in

Nuclear Medicine Review 2013, Vol. 16, No. 1

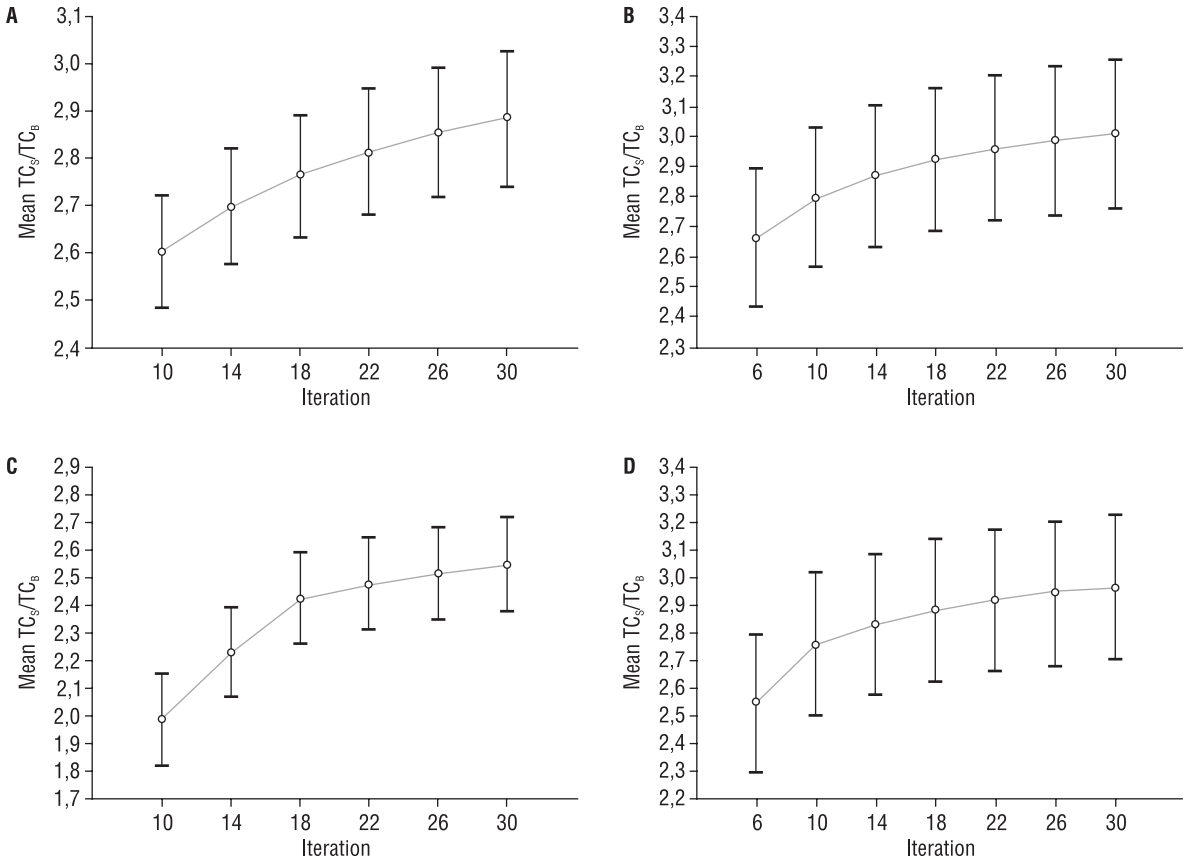

Figure 1. The mean value of the TC_S/TC_B ratio for a constant number of subsets (s = 8) and variable number of iterations (i): OSEM (8, i) for: **A.** small lesions localized in the liver, **B.** medium size lesions localized in the liver, **C.** small lesions localized outside the liver and **D.** medium size lesions localized outside the liver

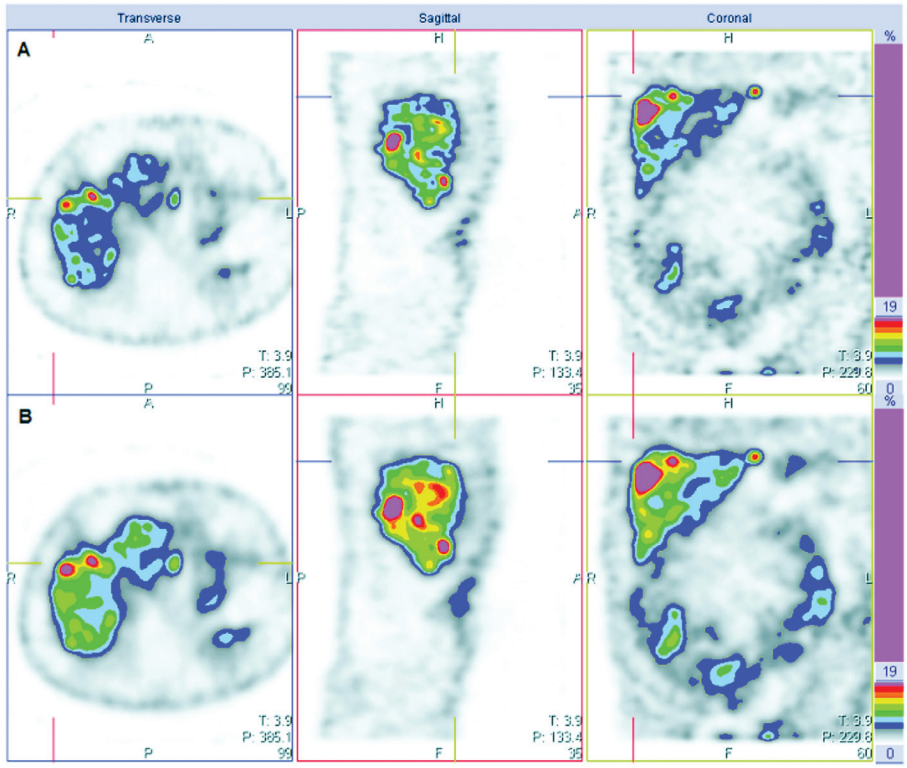

Figure 2. The effect of Gauss filtering FWHM = 4 mm (A) and FWHM = 8 mm (B) on the SRS image reconstructed with the OSEM algorithm (10 iterations for 8 subsets)

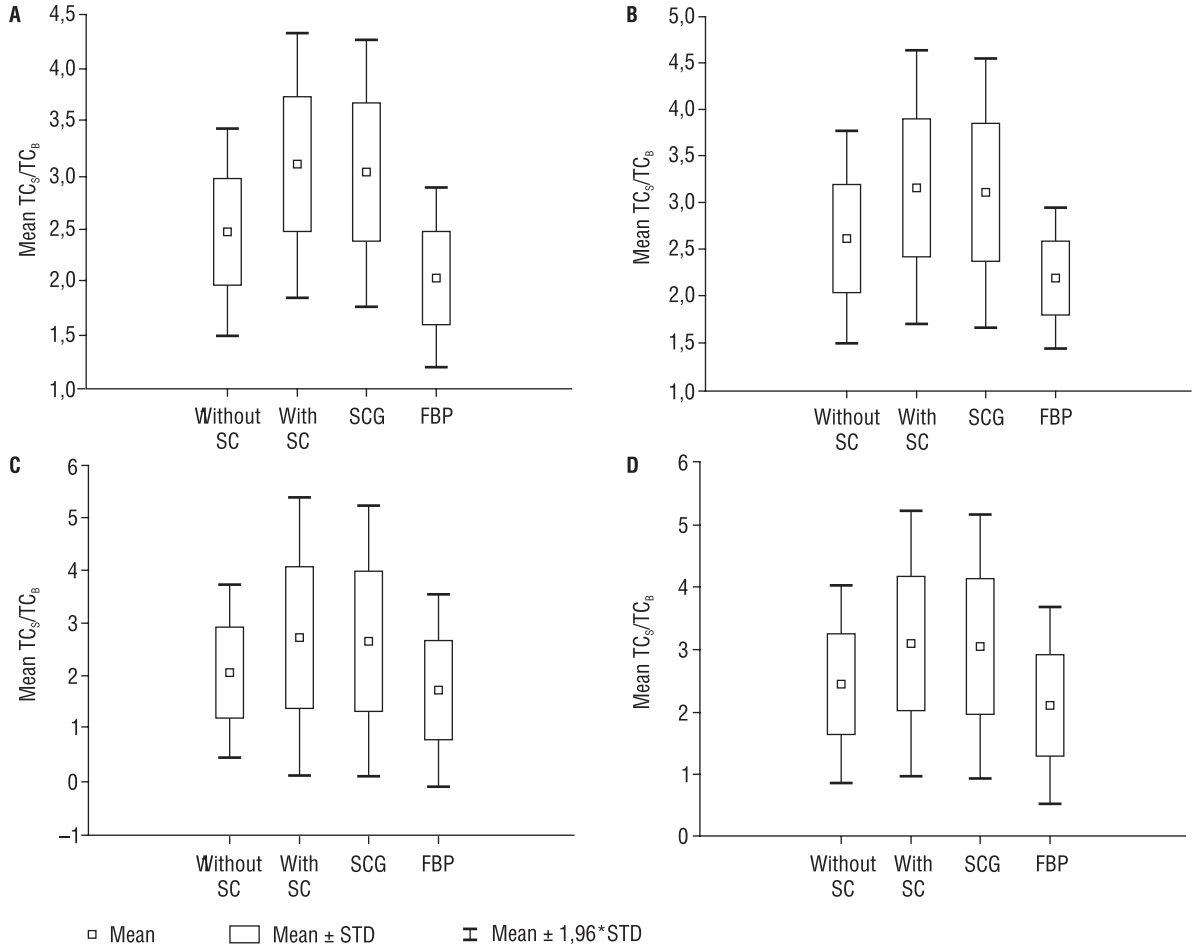

Figure 3. The mean value of the TC_S/TC_B ratio comparable to the most effective parameters of reconstruction OSEM (8, 10): with SC, without SC, with SC and Gauss Filter (FWHM = 4) *v.* FBP (Butterworth filter, fc = 0,86) for: **A.** small lesions localized in the liver, **B.** medium size lesions localized in the liver, **C.** small lesions localized outside the liber and **D.** medium size lesions localized outside the liver

quality assessment between images reconstructed with use of OSEM and FBP technique.

These quantitative results of the analysis of reconstructed clinical SPECT images were confirmed in the phantom study. The mean value of TC_S/TC_B ratio increased with number of iterations: from 1.47 to 2.61 and from 1.39 to 2.13 for low (4.7 kBq/ml) and high (37 kBq/ml) background activity concentration, respectively. Comparable to clinical study the highest value of TC_S/TC_B ratio was for optimized setting OSEM (8, 10) with SC for both background activity concentrations (Figures 5 and 6).

Discussion

In the analysis of SRS SPECT images with the use of labeled somatostatin analogs in patients with NETs it is important to optimize parameters of the OSEM reconstruction, because the choice of these parameters significantly influences not only the quality of SPECT images, but also quantitative assessment of the lesion signal to noise ratio, which is an important indicator used in the NET restaging [10].

In our opinion, the most crucial parameters of the OSEM algorithm are numbers of subsets and iterations. Based on the results of this study, we found that when using Flash 3D™ software the most effective combination is 10 iterations and 8 subsets. Additionally, for small lesions localized in the liver 10, 14 and 18 iterations provided similarly satisfying results. These outcomes are compatible with other authors' reports [11, 12, 18, 19, 21–26]. The OSEM Flash 3D™ is a sophisticated reconstruction algorithm which additionally includes 3D resolution recovery correction (transversal and axial) [18–20]. Therefore lesion signal to noise ratio obtained with the use of OSEM Flash 3D™ algorithm can be different than the ratio obtained when using a conventional iterative algorithm OSEM without resolution recovery.

Brambilla et al. investigated the usefulness of OSEM 3D algorithm in SPECT studies with ^{99m}Tc labeled compounds taking into account three parameters: the noise, the contrast and the spatial resolution [11]. Each parameter was analyzed in regard to varying numbers of subset and iteration. This study was performed with Jaszczak phantom (Jaszczak Deluxe ECT) using acquisition parameters typical for brain and myocardial examinations. The images obtained from the reconstructions performed with an optimized set of OSEM algorithm parameters were compared to those reconstructed using FBP method. Authors reported that the optimal number of subsets was 8 (128 × 128 matrix with 128 recorded projections). For different background activity concentrations the most effective combinations of subsets and iterations were 5 itera-

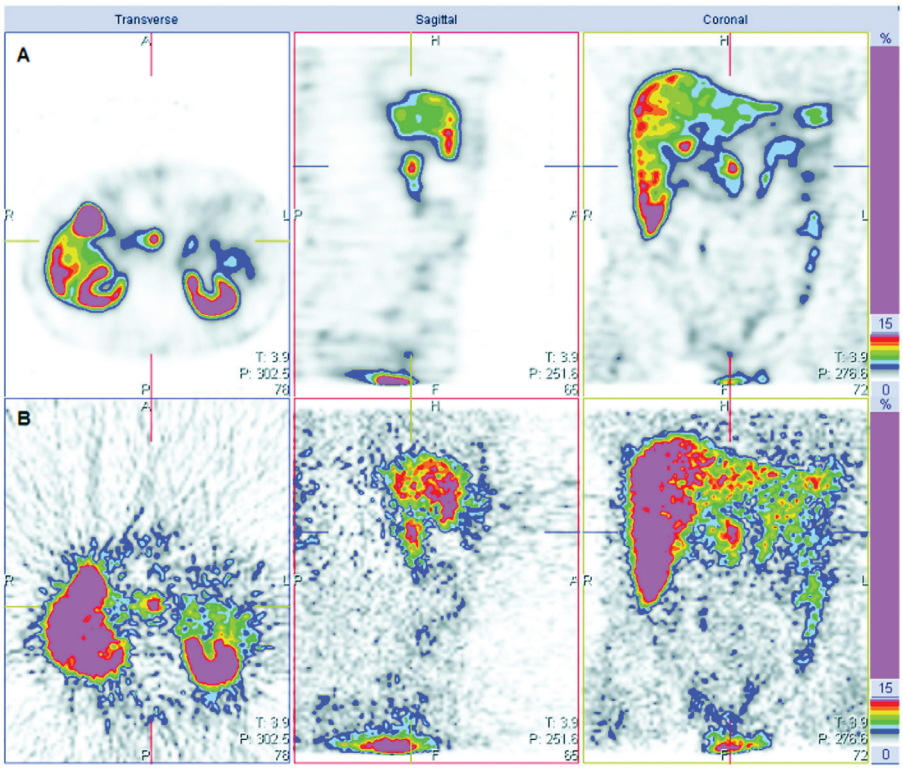

Figure 4. Differences in image quality between images reconstructed with OSEM (**A**) and FBP techniques (**B**)

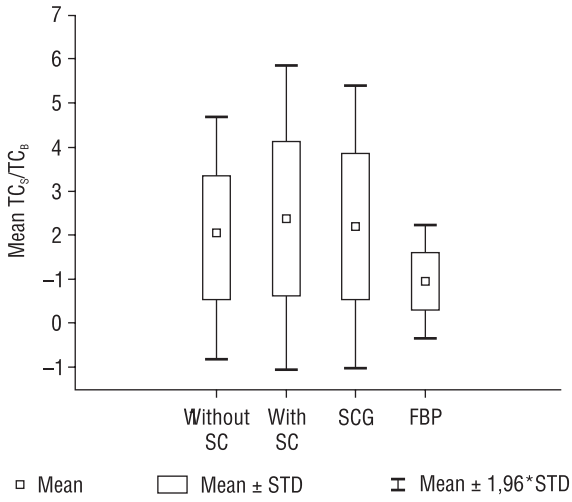

Figure 5. The mean value of the TC_S/TC_B ratio for the low background activity (phantom study). Comparison the most effective parameters of reconstruction OSEM (8,10) *v.* FBP

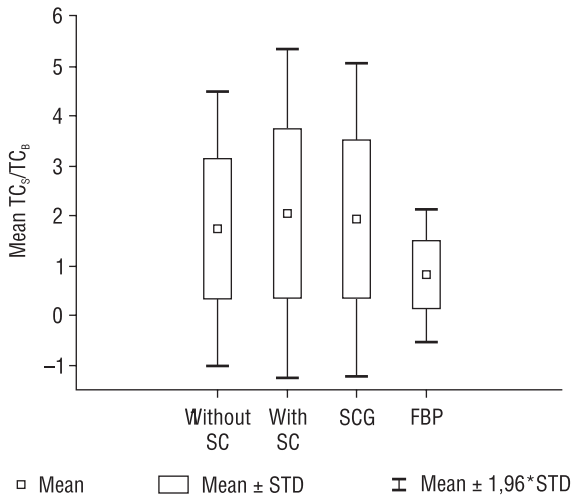

Figure 6. The mean value of the TC_S/TC_B ratio for the high background activity (phantom study). Comparison the most effective parameters of reconstruction OSEM (8, 10) *v.* FBP

tions for 8 and 4 subsets. Additionally, for high background activity 10 iterations for 8 subsets also gave satisfying results.

Blocklet et al. analyzed the OSEM 2D algorithm in comparison to FBP technique in bone SPECT (with used ^{99m}Tc-MDP) [12]. The authors used 2 iterations for 8 subsets for 64x64 matrix with 64 recorded projections. According to the results of our preliminary study (not included in that paper), these reconstruction settings were assessed as the most effective. Authors emphasized the fact that when increasing number of iterations the reconstruction time may also increase. But it should be taken into consideration that the reconstruction time strongly depends on a computer power. In our case, the reconstruction time (Fujitsu — Siemens Syngo MI Workplace, 128 × 128 matrix with 128 projections,) ranged from 30 seconds (6 iterations) to 90 seconds for the highest number of iterations (30 iterations). The image reconstruction with the use of OSEM (8, 10) takes approximately 35 seconds.

Scatter correction (SC) application slightly improved image quality for small and medium size lesions detected in the extrahepatic lesion localized within the abdomen. But for lesions detected in the liver reconstruction with or without SC did not influence the quality

of SPECT images. However, in a quantitative assessment for both localizations SC improves lesion signal to noise ratio. Opinions about the influence of SC on the quality of reconstructed image are divided. Benefits of this tool depend on the respective localizations of healthy organs and pathological lesions. Starck et al. evaluated the influence of SC on image contrast for SPECT examination of the spine (bone scintigraphy with ^{99m}Tc-MDP) [21]. In this study only a qualitative assessment was performed by five independent observers. According to their opinion SC did not improve image quality when compared to images reconstructed without SC. However, other authors reported opposite results. Hayashi et al. compared different methods of attenuation and scatter corrections in SPECT study of the brain perfusion [22]. In this study the utilization of SC reduced an overestimation of regional cerebral blood flow (CBF) in a low-flow region. Vines et al. used the striatal phantom for the evaluation of SC method in a quantitative brain SPECT study [23]. Measured striatal-to-background ratios were underestimated on average by approximately 41% compared to expected ratios in images reconstructed without SC. Therefore, the differences in quality assessment between lesions localized in the liver and outside the liver that were found in our study are justified. The quality of the reconstructed image for extrahepatic lesions localization improves due to low counts statistic in the near background.

In our study, the optimal settings of Gaussian filter corresponded to FWHM = 4mm or 8mm and depended on the localization and the size of lesions. These FWHM values were equal to pixel size and double pixel size, respectively. However the utilization of Gauss filter is not necessary and may in some cases be detrimental to the image quality. First of all, image smoothing will not improve the quality of reconstructed image if the number of subsets and iterations are properly chosen. Moreover, the value of TC_S/TC_B ratio decreases with increasing FWHM value of the filter coefficient for both considered localization and regardless of lesions size. SPECT image reconstructed with the use of OSEM algorithm without smoothing filter will have better spatial resolution and contrast [11]. Contrast and TC_S/TC_B ratio increase with increasing number of iterations. However, for low statistics data images reconstructed with more iterations may include much more noise. In this case, noise reduction is possible with smoothing filter, but at the cost of resolution deterioration [10].

It is expected that in the near future iterative algorithms will replace FBP technique leading to better physical representation of organs and pathological lesions in the reconstructed images. Also, reasonably fast time of reconstruction will be an important factor (less than 2 minutes) [18]. In this study, authors clearly show that iterative method (OSEM) is a better choice for SRS SPECT image reconstruction. For small and medium size lesions localized in the liver many more of them were assessed as very well visible (31% *v.* 8% and 54% *v.* 11%, respectively). Comparable results were observed for extrahepatic lesions (15% *v.* 10% and 82% *v.* 42%, respectively). Many papers emphasized a superiority of iterative technique over FBP method in SPECT images reconstruction [18, 19, 24, 25]. It is related to the absence of streak artifacts of FBP technique [26]. Divoli et al. investigated variations and reproducibility in the estimated absorbed dose owing to different reconstruction algorithms (OSEM *v.* FBP) [27]. The utilization of different reconstruction algorithms can result in differences higher than 50% in estimated tumor absorbed doses. Therefore standardization of the reconstruction methodology is necessary in tumor dosimetry, especially when data are collected by many different centers. In our case, this standardization is very important, because of the assessment of disease progression when the SRS study is evaluated before and after PRRT.

For the phantom study, only the quantitative assessment was performed. The TC_S/TC_B ratio was analyzed. Similarly to the clinical part of our study, TC_S/TC_B ratio increased with increasing number of iterations for both high and low background activity. The most variation for low and high background activity was found for 8 and 16 subsets with different number of iterations and 8 subsets with different number of iterations, respectively. However, the phantom studies cannot be used as the final indicator in clinical practice. They might only be used to confirm the choice of the reconstruction parameters and perform quantitative analysis of the results. Reconstruction parameters determined based on phantom studies always require verification in clinical experiments. In order to decide if the choice of reconstruction technique and its parameters are appropriate, a clinical study must be performed [28].

Conclusions

OSEM (8, i) is the most effective setting of reconstructions parameters of the iterative algorithm OSEM Flash 3D (Siemens) for 128 recorded/acquired projections. Especially, OSEM (8, 10) setting gives the best results in the qualitative assessment of SRS study with the use of SPECT technique. Application of scatter correction slightly improves quality of images and increases the value of lesion signal to noise ratio. Application of Gauss post-filtering degrades the contrast but did not affect the high quality of images. However, this result applies only if Gauss filter's FWHM coefficient does not exceed a double value of the pixel size. Generally, iterative technique (OSEM Flash 3D algorithm) gives better outcomes for both the qualitative and quantitative assessment of SRS SPECT studies in comparison to FBP method. The choice of reconstruction parameters is the most important thing in the evaluation of small and middle-size lesions. In case of large lesions, especially when there are assessed by experienced clinician, the choice of reconstruction parameters does not influence the diagnostic assessment of received SPECT images.

The authors have nothing to disclose.

References

1. Pepe G, Moncayo R, Bombardieri E et al. Somatostatin receptor SPECT. Eur J Nucl Med Mol Imaging 2012; 39 (Suppl 1): S41–S51.
2. Bombardieri E, Coliva A, Maccauro M et al. Imaging of neuroendocrine tumours with gamma-emitting radiopharmaceuticals. Q J Nucl Med Mol Imaging 2010; 54: 3–15.
3. Apostolova I, Riethdorf S, Buchert R et al. SPECT/CT stabilizes the interpretation of somatostatin receptor scintigraphy findings: a retrospective analysis if inter-rater agreement. Ann Nucl Med 2010; 24: 477–483.
4. Balon HR, Goldsmith SJ, Siegel BA et al. Procedure guideline for somatostatin receptor scinitgraphy with (111) In-pentetrotide. J Nucl Med 2001; 42: 1134–1138.
5. Gotthardt M, Dirkmorfeld LM, Wied MU et al. Influence of somatostatin receptor scintigraphy and CT/MRI on the clinical management of patients

with gastrointestinal neuroendocrine tumors: an analysis in 188 patients. Diegstion 2003; 68: 80–85.
6. Krausz Y, Israel O. Single-photon emission computed tomography/computed tomography in endocrinology. Semin Nucl Med 2006; 36: 267–274.
7. Schillaci O, Spanu A, Scopinaro F et al. Somatostatin receptor scintigraphy with 111In-pentetreotide in non-functioning gastroenteropancreatic neuroendocrine tumors. Int J Oncol 2003; 23: 1687–1695.
8. Jarząb B, Handkiewicz-Junak D. Guzy neuroendokrynne — część I. Najważniejsze zasady diagnostyki i leczenia w świetle aktualnych rekomendacji Polskiej Sieci Guzów Neuroendokrynnych. Medycyna Praktyczna Onkologia 2009; 5: 29–39.
9. Hudson HM, Larkin RS. Accelerated image reconstruction using ordered subsets of projection data. IEE Trans Med Imaging 1994; 13: 601–609.
10. Gutman F, Gardin I, Delahaye N et al. Optimisation of the OS-EM algorithm and comparison with FBP for image reconstruction on a dual-head camera: a phantom and clinical ^{18}F-FDG study. Eur J Nucl Med Mol Imaging 2003; 30: 1510–1519.
11. Brambilla M, Cannillo B, Dominietto M et al. Characterization of ordered-subsets expectation maximization with 3D post-recostruction Gauss filtering and comparison with filtered backprojection in ^{99m}Tc SPECT. Ann Nucl Med 2005; 19: 75–82.
12. Blocklet D, Seret A, Popa N et al. Maximum-likelihood reconstruction with ordered subsets in bone SPECT. J nucl Med 1999; 40: 1978–1984.
13. Case JA, Licho R, King MA et al. Bone SPECT of the spine: a comparison of attenuation correction techniques. J Nucl Med 1999; 40: 604–613.
14. Kauppinen T, Koskinen MO, Alenius S et al. Improvement of brain perfusion SPET using iterative reconstruction with scatter and non-unifom attenuation correction. Eur J Nucl Med 2000; 27: 1380–1386.
15. Vanhove C, Defrise M, Franken PR et al. Interest of ordered subsets expectation maximization (OS-EM) algorithm in pinhole single-photon emission tomography reconstruction: a phantom study. Eur J Nucl Med 2000; 27: 140–146.
16. Wells GR, King MA, Simkin PH et al. Comparing filtered backprojection and ordered-subsets expectation maximization for small-lesion detection and localization in ^{67}Ga SPECT. J Nucl Med 2000; 41: 1391–1399.
17. Chang LT. A method for attenuation correction radionuclide computed tomography. IEEE Trans Nucl Sci 1978; 25: 638–643.
18. Römer W, Reichel N, Vija HA et al. Isotropic reconstruction of SPECT data using OSEM 3D: correlation with CT. Academic Radiology 2006; 13: 496–502.
19. Vija AH, Hawman EG, Engdahl JC. Alaysis of SPECT OSEM reconstruction method with 3D beam modeling and optional attenuation correction: phantom studies. IEEE Nuclear Science Symposium, Medical Imaging Conference, Portland, USA, 19–25.10.2003; conference record: 2662–2666, ISBN: 0–7803–8257–9.
20. Zeintl J, Hans Vija A, Yahil A et al. Quantitative accuracy of clinical ^{99m}Tc SPECT/CT using ordered-subset expectation maximization with 3-dimensional resolution recovery, attenuation, and scatter correction. J Nucl Med 2010; 51: 921–928.
21. Starck SA, Ohlsson J, Carlsson S. An evaluation of reconstruction techniques and scatter correction in bone SPECT of the spine. Nucl Med Communications 2003;24:565-570.
22. Hayashi M, Deguchi J, Utsunomiya K et al. Comparison of methods of attenuation and scatter correction in brain perfusion SPECT. J Nucl Med Technology 2005; 33: 224–229.
23. Vines DC, Ichise M, Liow JS et al. Evaluation of 2 scatter correction methods using a striatal phantom for quantitative brain SPECT. Mol Imaging Branch 2003; 31: 157–160.
24. Lappi S, Lazzari S, Sarti G et al. Assessment of geometrical distortion and activity distribution after attenuation correction: a SPECT phantom study. J Nucl Cardiol 2002; 9: 508–514.
25. Yokoi T, Shinohara H, Onishi H. Performance evaluation of OSEM reconstruction algorithm incorporating three-dimensional distance-dependent resolution compensation for brain SPECT: a simulation study. Ann Nucl Med 2002; 16: 11–18.
26. Cherry SR, Sorenson JA, Phelps ME. Physics in nuclear medicine. Third edition. Elsevier 2003.
27. Divoli A, Bloch G, Chittenden S et al. Tumor dosimetry on SPECT (186) Re-HEDP scans: variations in the results from reconstruction methods used. Cancer Biother Radiopharm 2007; 22: 121–124.
28. Lalush DS, Tsui BM. Performance of ordered-subset reconstruction algorithms under conditions of extreme attenuation and truncation in myocardial SPECT. J Nucl Med 2000; 41: 737–744.